Electronic Supplementary Material (ESI) for Soft Matter.

Electronic Supplementary information for

Phase behaviour in 2D assemblies of dumbbell-shaped colloids generated under geometrical confinement

*Rouven Stuckert[‡a], Anton Lüders[‡b], Alexander Wittemann[*a] und Peter Nielaba[*b]*

[a] Colloid Chemistry, Department of Chemistry, University of Konstanz, Universitaetsstrasse 10, 78464 Konstanz, Germany. Correspondence: alexander.wittemann@uni-konstanz.de; Tel.: +49-(0)7531-88-5458.

[b] Statistical and Computational Physics, Department of Physics, University of Konstanz, Universitaetsstrasse 10, 78464 Konstanz, Germany. Correspondence: peter.nielaba@uni-konstanz.de.

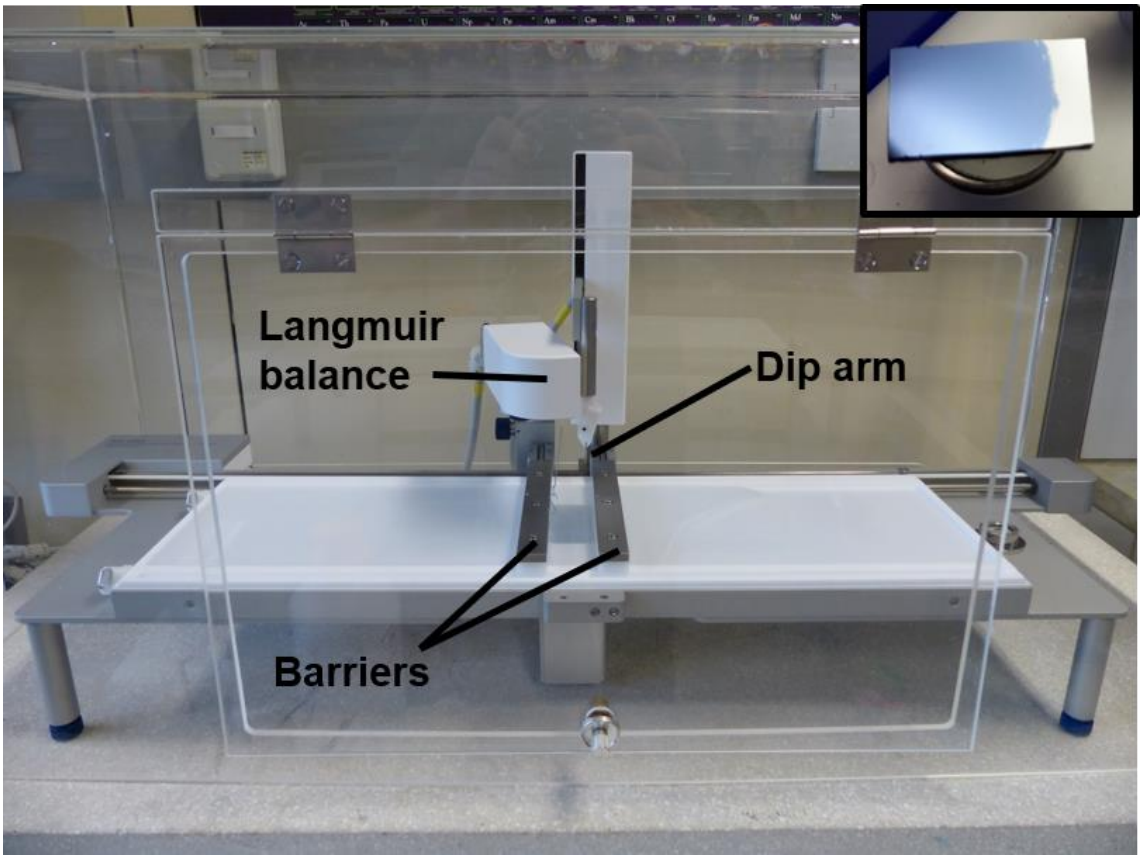

Figure S1. Langmuir-Blodgett setup used for assembly of dumbbell particles. Inset shows a dried monolayer of dumbbell particles transferred to a Si wafer.

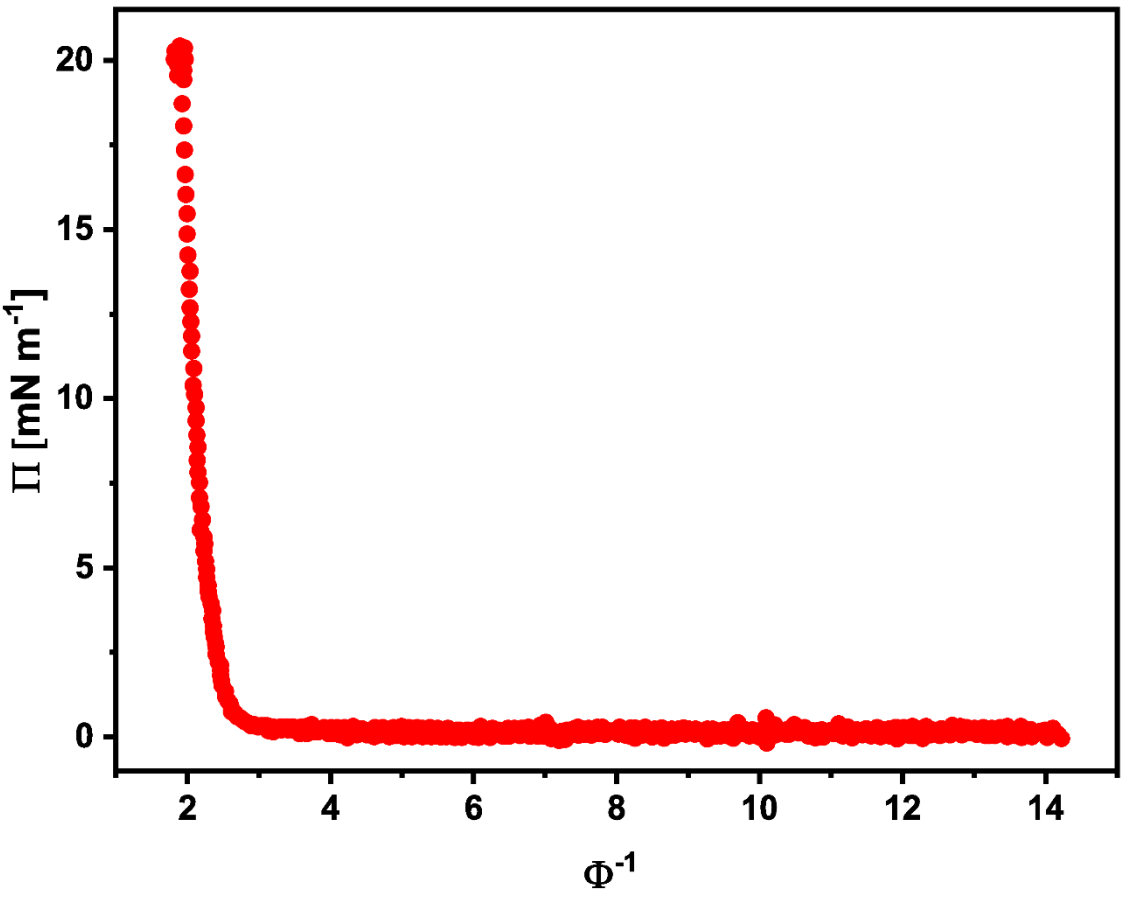

Figure S2. Surface pressure (Π) plotted against the reciprocal value of the area fraction (Φ^{-1}) of a dumbbell particle monolayer transferred at 20 mN m^{-1}. The surface pressure was measured utilizing a Wilhelmy plate. The reciprocal area fraction was calculated from the average cross-section of the dumbbell particles immersed half its height into water, corresponding to a contact angle of 90° at the air/water interface. The experiment was performed at 25°C.

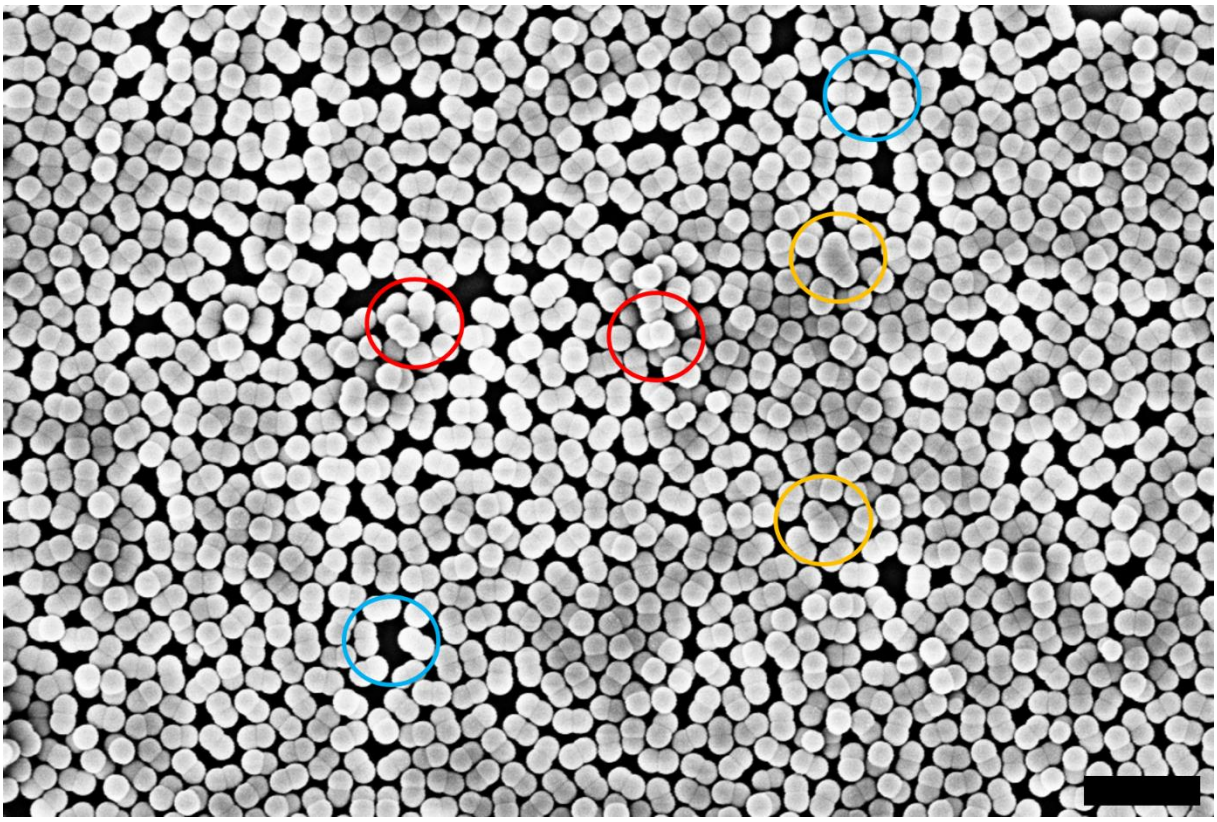

Figure S3. Examples of defects in monolayers of dumbbell particles transferred to a Si wafer. **Red circles:** Out-of-plane particles. **Orange circles:** Higher-order species obtained as a side product during synthesis. **Light blue Circles:** Vacancies/Loose packing. Scale bar: 500 nm.

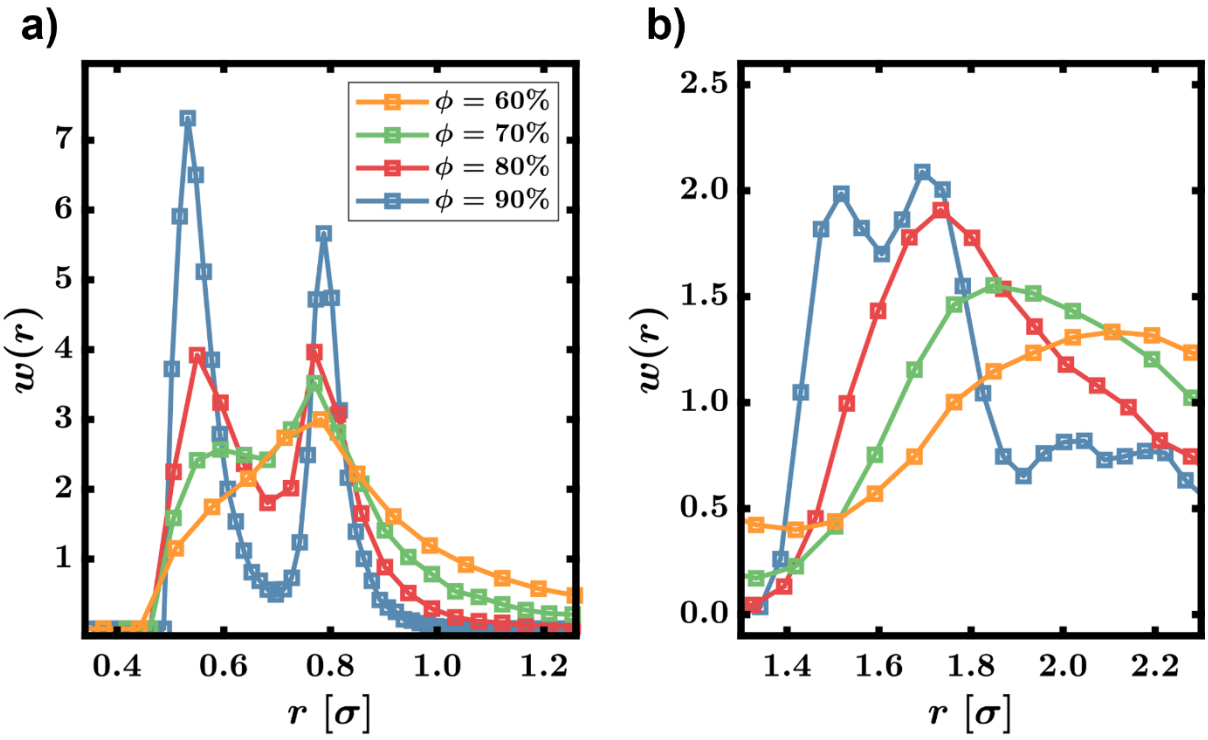

Figure S4. Particle distribution close to the barriers: The experimental Langmuir-Blodgett assembly is not suited to transfer films very close to the barriers and thus the influence of the wall on the particle distribution cannot be evaluated by our experiments. Simulations however, enable predictions regarding the particle density near the barriers. The quantity $w(r)$ is the density function corresponding to the probability of finding a particle at distance r from the barriers normalized by the value expected for an ideal gas. Therefore, $w(r)$ matches the pair correlation functions $g(r)$ used to describe the structure of the monolayers. The particle distribution is compared for systems with different area fractions Φ. The colors are matched between both figures. **a)** Particle distribution for small distances r. By enhancing Φ, a sharp particle distribution results which is characterized by two distinct peaks. The first peak corresponds to particles which are oriented parallel to the barriers and the second peak corresponds to particles with an orientation perpendicular to the walls. The sharp progression of the distribution indicates a dominant local order near the barriers which becomes especially noticeable at high area fractions. **b)** Particle distributions in the vicinity of a distance $r = 1.8$ from the barriers. Here as well, the distribution becomes sharper at higher area fractions. By enhancing the area fractions, distinct features arise which point to a high local order close to the barriers.

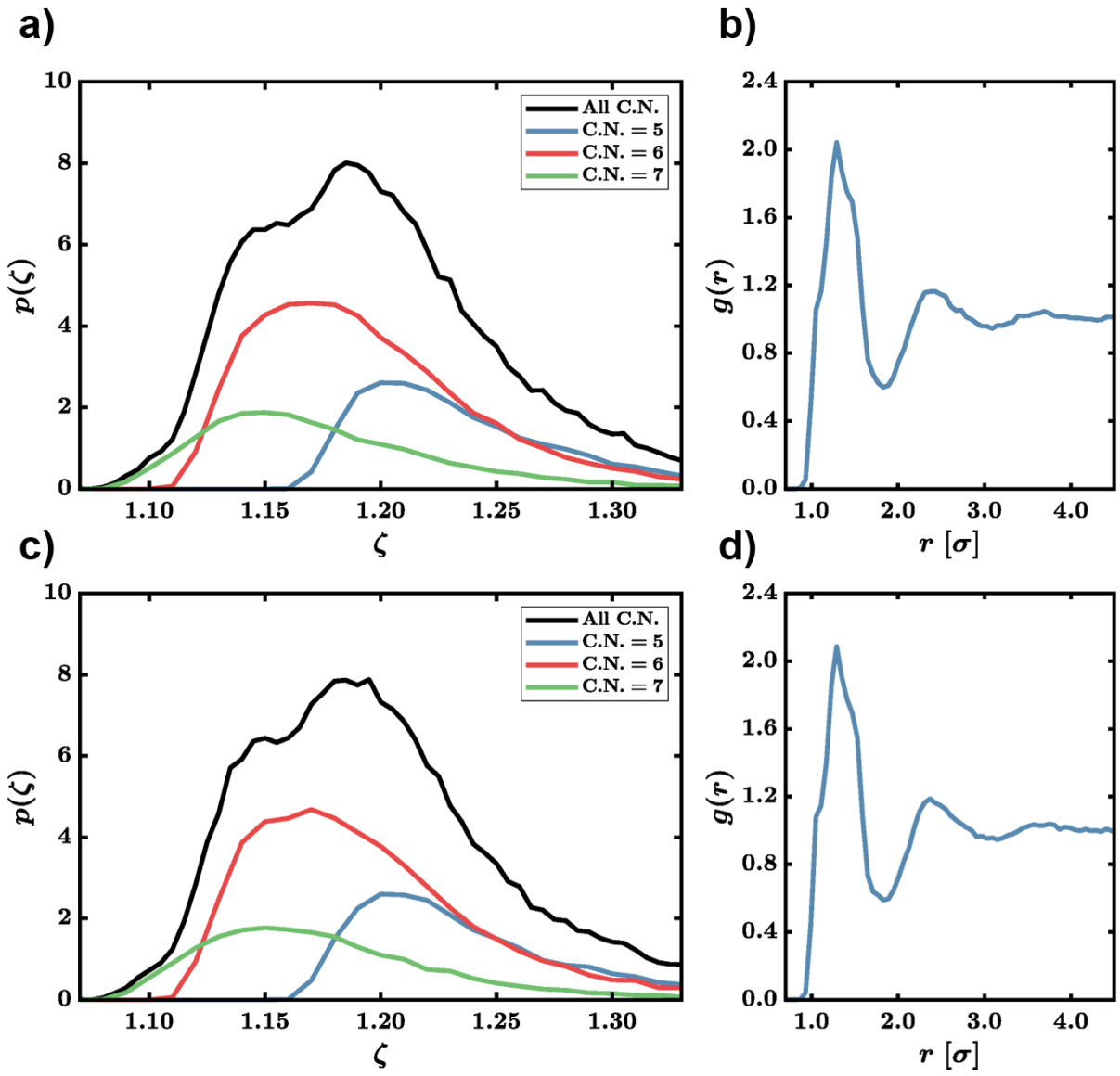

Figure S5. Quantitative analysis of transfer rate on the resulting experimental dumbbell monolayer. **a)** Probability densities of the shape factor of the Voronoi tessellation from monolayers transferred at 0.1 mm min^{-1}. **b)** Pair correlation function calculated from the center of mass of the dumbbell particles from monolayers transferred at 0.1 mm min^{-1}. **c)** Probability densities of the shape factor of the Voronoi tessellation from monolayers transferred at 10 mm min^{-1}. **d)** Pair correlation function calculated from the center of mass of the dumbbell particles from monolayers transferred at 10 mm min^{-1}. Target surface pressure was set to 20 mN m^{-1} for all experiments. No significant difference can be seen from variation in the transfer speed in either the probability of shape factors or the pair correlation functions in these experiments.

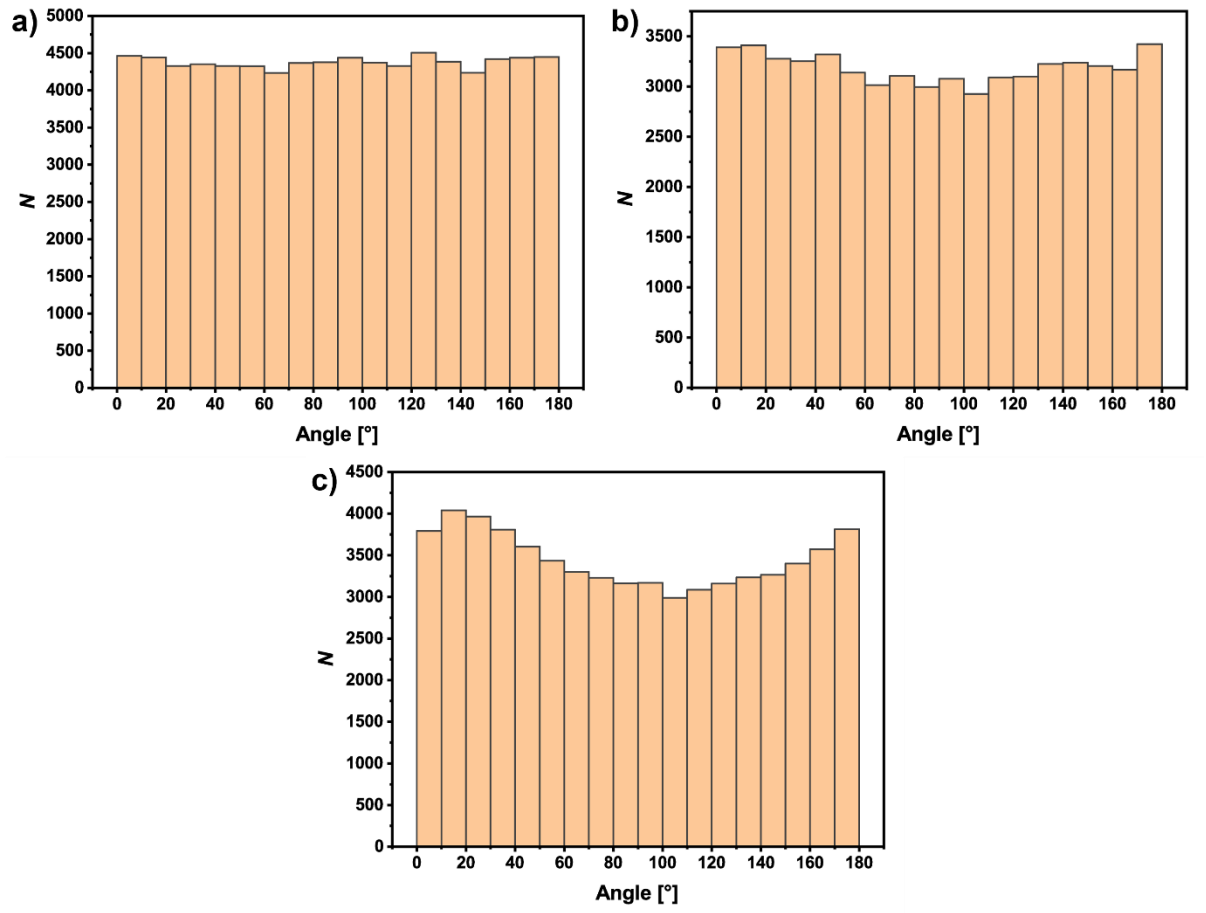

Figure S6. Angle distributions of dumbbell particles assembled into monolayers at different final area fractions. The data are obtained by evaluating FESEM micrographs, in which the horizontal direction is aligned parallel to the barriers. Particles oriented with their long axis along the horizontal of the image therefore possess an angle of 0° or 180°. The image horizontal also coincides with the lift-off direction of the substrate during Langmuir-Blodgett transfer of the monolayer. The receding meniscus at the substrate is thus perpendicular to this direction.

a) 15mN m^{-1}, Φ = 67%. The lack of distinct features in the distribution indicates the absence of preferential orientation towards the horizontal if averaged over a large number of domains. **b)** 20mN m^{-1}, Φ = 70%. A preferential orientation is barely visible. **c)** 30mN m^{-1}, Φ = 76%. A slight preference for the direction of the lift-off is seen from the distribution. The effect is however rather small.

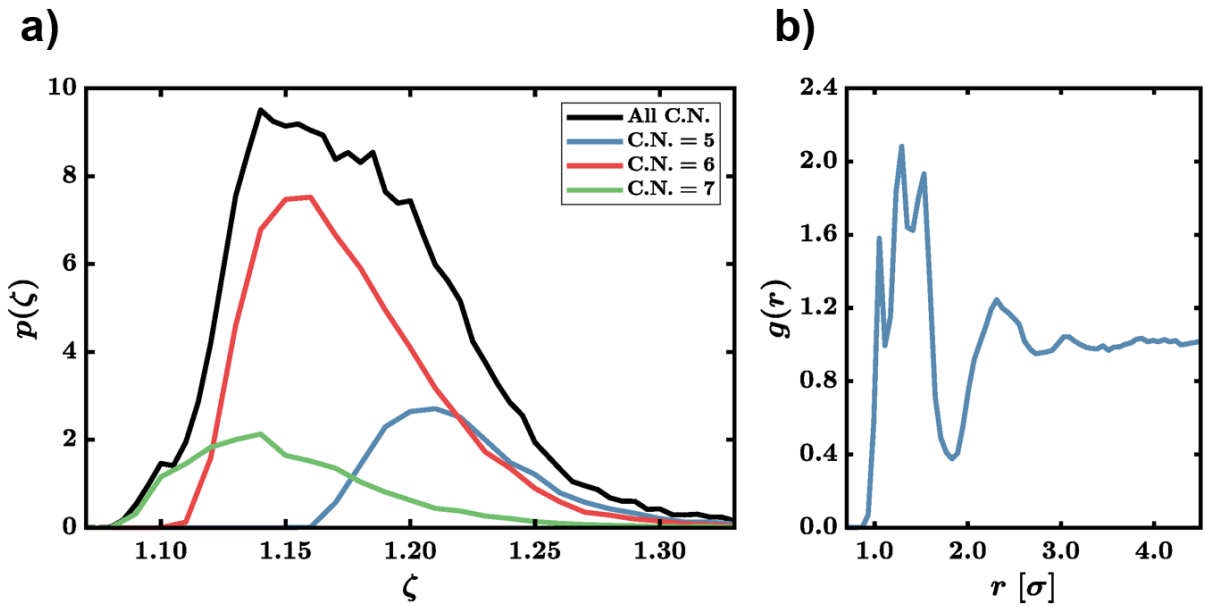

Figure S7. Quantitative analysis of dumbbell monolayers assembled *via* drying mediated assembly with an area fraction of 80%. **a)** Probability densities of the shape factors of the Voronoi tessellation. **b)** Pair correlation function based on the centers of mass of the dumbbell particles.

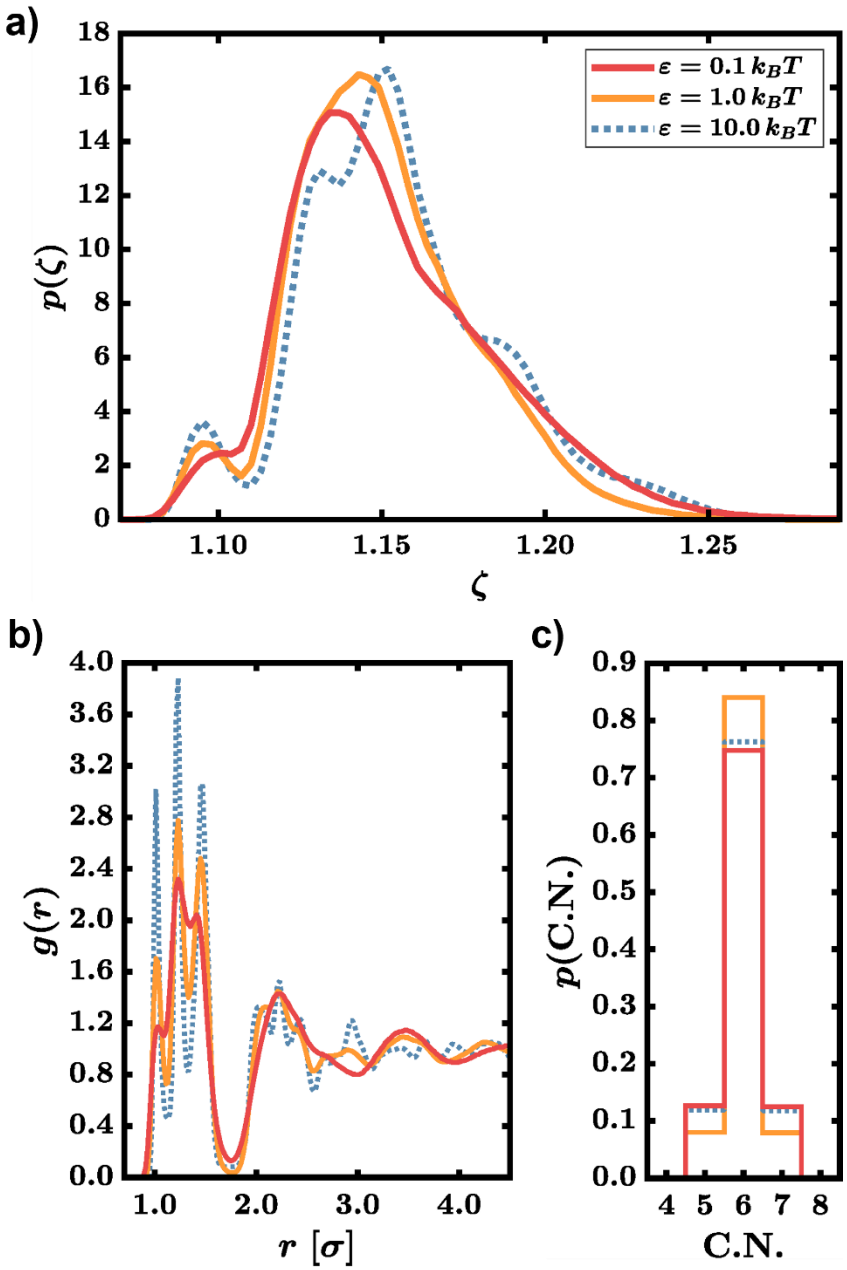

Figure S8. Quantitative analysis of simulated dumbbell monolayers at a final area fraction of Φ = 90 % and different interaction strengths ε. The colours of the curves are matched between the figures a), b) and c). The barrier speed is 7.86 σ/τ_D. The curves for ε = 0.1 k_BT are generated using 393 simulations which were equilibrated for 1000 τ_D, the curves for ε = 1.0 k_BT are based on 590 simulation which were equilibrated for at least 730 τ_D and the curves for ε = 10.0 k_BT are calculated using 615 simulations which were equilibrated for at least 730 τ_D. All results suggest that a change in the interaction strength affects systems with higher area fractions at a larger extent. **a)** Probability density $p(\zeta)$ of the shape factor ζ at different interaction strengths. Changing the interactions strength from ε = 0.1 k_BT to ε = 1.0 k_BT, the dominant peak of the

progression of $p(\zeta)$ increases noticeably. For ε = 10.0 k_BT, the system enters a new regime in which the probability density of ζ develops a sharp substructure. This indicates a monolayered superstructure in which the possible shapes of the Voronoi cells are rather uniform or similar to each other and less continuously distributed. **b)** Pair correlation functions $g(r)$ at different interaction strengths. By increasing the interaction strength, the substructure of the first maxima sharpens to three distinct peaks. This is in line with the pair correlation function of the monolayer generated *via* drying mediated assembly which is depicted in Fig. S5. The pair correlation function for ε = 10.0 k_BT possesses multiple local maxima and minima throughout the depicted r interval. **c)** Probability distribution of the coordination number C.N. for different interaction strengths. Increasing ε from ε = 0.1 k_BT to ε = 1.0 k_BT leads to a higher percentage of particles with six nearest neighbours. Interestingly, this percentage declines, if the interaction strength increased to ε = 10.0 k_BT. A possible explanation for this phenomenon could be the decreasing particle mobility in the monolayers: By increasing the area fraction and the interaction strength, the particle mobility in the monolayers decreases significantly. At a certain point, the motion of the particles could be hindered to an extent that they cannot align. Therefore, the monolayer remains in the state the system enters immediately after the final area fraction is reached and the particles occupy the whole simulation box. In systems with smaller ε, the resulting structures are more homogeneous due to the mobility of the particles while the system is equilibrated. Here, more non-uniform Voronoi cells with six vertices can form.